PAPER • **OPEN ACCESS**

High-resolution Interferometric Measurement of Thickness Change on a Lithium-Ion Pouch Battery

To cite this article: G Bohn *et al* 2019 *IOP Conf. Ser.: Earth Environ. Sci.* **281** 012030

High-resolution Interferometric Measurement of Thickness Change on a Lithium-Ion Pouch Battery

G Bohn[1], J Taub[1], A Linke[1, 2], S Bayer[3], D Oeser[1, 2], A Ziegler[1, 2], P Ettl[4] and A Ackva[1, 2]

[1]Faculty of Electrical Engineering, University of Applied Sciences Würzburg/Schweinfurt, 97421 Schweinfurt, Germany
[2]Technologie-Transfer-Zentrum-Elektromobilität, University of Applied Sciences Würzburg/Schweinfurt, 97616 Bad Neustadt, Germany
[3]Staatliches Bauamt, Weißenburgstraße 6, 97082 Würzburg, Germany
[4]3D-Shape GmbH, Am Weichselgarten 21, 91058 Erlangen, Germany

Gunther.bohn@fhws.de

Abstract: Volume change of graphite leads to change in thickness of battery storage layers during discharging and charging. Pouch cell lithium ion batteries are used in the field of electric vehicles and solar home storage. This paper shows a measurement setup for the three-dimensional measurement of thickness change on a flat 6.7mm thick pouch cell using a white light interferometer. With a measuring field of 7.05mm diameter the resulting 3D thickness change record contains 226000 3D readings. The measuring points have a lateral distance of 13.1µm. The repeatability of the measurement is 312.8nm for the individual values and 64.1nm for the average value. In addition, this paper shows how the storage capacity of this pouch cell drops over 30 charge cycles.

1. Introduction

Lithium-ion batteries [1]-[2] combined with low-carbon power generation will make it possible to greatly reduce CO_2 emissions in many areas, such as traffic or lighting. In these applications pouch cells have great potential due to their low production costs [3]. They are used in various types of electric vehicles [4]. For most types of lithium ion batteries, graphite is used as storage for lithium in the anode. Graphite is inexpensive and allows high cycle stability. Figure 1 shows the active layers in a lithium cobalt oxide battery. Layers are aluminum, lithium cobalt oxide, separator, graphite and copper. Aluminum and copper serve as current conductors. To increase the storage capacity, the layers are wound (cylindrical design), folded or stacked (flat prismatic design or pouch cell design).

Production of lithium ion batteries requires 70kg of CO_2 per kWh storage capacity at the current state of the art [5]. Therefore, the lifetime of the accumulators is crucial for the CO_2 balance of their use [6]. Change in volume of graphite during charging and discharging of the accumulator together with other factors such as SEI film growth leads to the limitation of the lifetime of the accumulator [7].

When a lithium ion battery with graphite anode is charged from 0% to 100% state of charge, the thickness of the graphite layer increases by up to 10%. The reason is the intercalation of lithium atoms in the crystal matrix of graphite. This increases the distance between the atom layers. During unloading, the thickness of the graphite layer shrinks again. Volume change of the graphite layer leads

to mechanical stress in the layers of the accumulator, cracking or change of the internal pressure in accumulators with a solid housing. As a result, the storage capacity of the accumulator decreases with each cycle of charging and discharging until the end of its life.

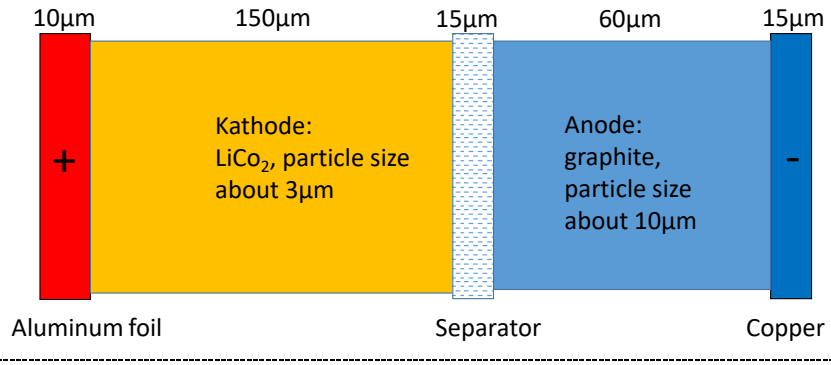

Figure 1. Layers of a lithium cobalt oxide accumulator with typical layer thickness [8].

Standard methods for measuring the volume change of graphite are XRD [9] and dilatometry [10]. In both methods, only the mean volume change of a large sample (e.g. area 300µm²) can be measured. In principle, interferometry enables length measurement with the highest precision [11]. A scanning white light interferometer with a 2D camera as a sensor also allows three-dimensional topology measurement [12]-[13].

In the lithium polymer accumulator, the electrolyte is bound in a solid or gelatinous polymer. This type of accumulator does not require a solid housing. In the pouch cell design, the active layers are packed in a flexible aluminum foil. As a result, the volume change of the graphite layer leads to a change in thickness of the accumulator, which can be measured from the outside.

2. Measurement setups

A standard lithium polymer accumulator in pouch design is the measuring object (Figure 2).

Figure 2. Measurement object (model 703759P-3.7V-2000mAh, manufacturer Shenzhen Xin Lian Xin Technology Co. Ltd.).

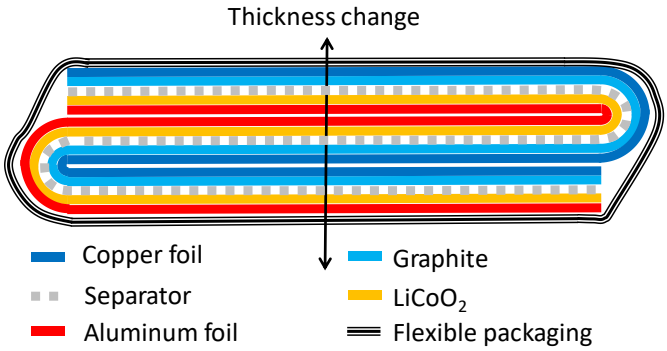

Figure 3. Layers in the pouch cell (folded three times) and thickness change of the cell. The layers can be folded many times. Example: Layers with a thickness of 200µm are folded 20 times. The total thickness is 4mm.

Its nominal capacity is 2000mAh. This cell has an internal battery protection circuit with discharge cut-off voltage 2.75V and charge cut-off voltage 4.2V. As a result, in the laboratory there is no risk of battery burn and pollution of the optical devices by smoke. The dimensions of the cell according to the

manufacturer are: thickness 6.5mm, length 63.6mm and width 39.5mm. The thickness of the fully charged cell is 6.6mm when measured with a vernier caliper.

2.1. Interferometric setup for thickness change during cyclization
The cell undergoes a cycle with 100% discharge and charge. Discharge time is 72 minutes and the charge time is 290 minutes. During this cycle, the surface of the cell is measured by the interferometer 74 times in three dimensions. Thickness change of the cell is determined from the 3D data by image processing.

2.1.1. Thickness change. In pouch design with folded layers (Figure 3), many copper and aluminum layers make the cell very stable in the direction parallel to the graphite layer. Therefore, a change in volume of the graphite mainly leads to a change in thickness of the graphite layers. Due to the flexible packaging, the internal thickness change of the graphite layers can be measured from the outside as a change in the thickness of the cell.

2.1.2. Optomechanical measurement setup. The battery is located in the object arm (Figure 4) of a scanning Michelson interferometer [14].

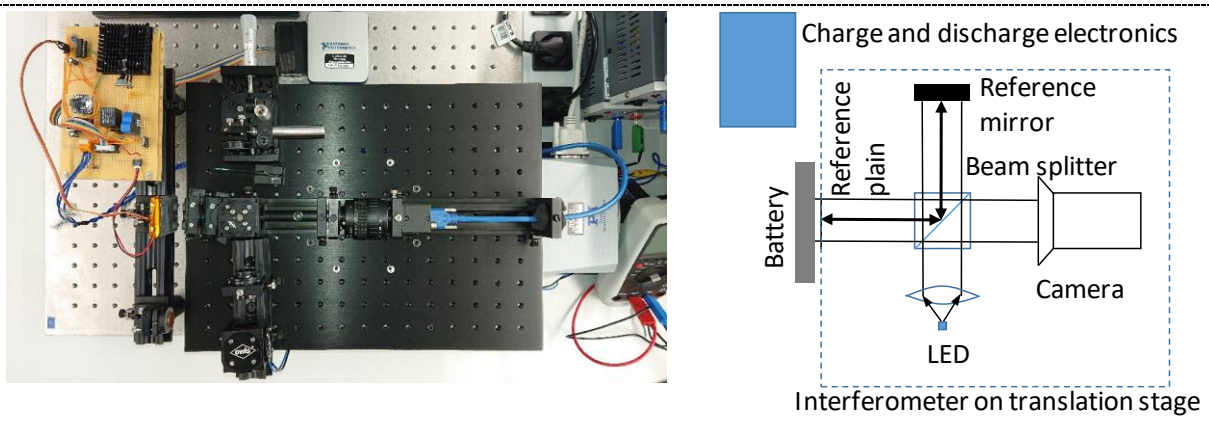

Figure 4. Picture and structure of the measurement setup.

A LED with a medium wavelength of 660nm and a bandwidth of 20nm is used as light source. A lens produces a plane wave from the light of the LED. The wave is split in the beam splitter. One part of the wave goes to the reference mirror and on to the camera. The other part of the wave passes over the measuring object to the camera. Interference only occurs if the optical path lengths in the reference path and object path are the same length. This defines the reference plane. During the measurement, the translation unit moves the interferometer assembly to the object at the scanning speed of 4.0µm/s against the Z direction (Figure 5). The reference plane moves slowly through the object. The camera and the connected image processing unit (software Softkorad, manufacturer 3D-Shape) detect the interference for each pixel and store the position of the translation unit as Z value [15]. At a scan speed of 4.0µm/s and a Z range of 500µm, the measurement time is 125 seconds.

In XY direction the measuring field is round with a diameter of 7.05mm. Limitations for the measuring field are the width of the beam splitter (10mm) and the diameter of the lenses used. In this measurement setup, the diameter is equivalent to 537 pixels of the camera. XY resolution is thus 13.12µm per pixel. Since each pixel of the camera can provide one Z value, the number of 3D values is up to 226000. By principle, however, there are pixels in the measurement for which no Z value can be determined. At the pixels where the target has wrinkles with steep edges, no light is reflected back to the camera. Then there will be no interference and the image processing of the interferometer cannot find a Z value. These pixels are filtered by the downstream 3D image processing. If pixels with

valid values can be found in the vicinity of a pixel without a valid Z value, a new Z value is assigned to the pixel. This value is the median of the Z values of the adjacent pixels with valid values.

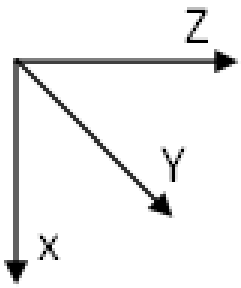

Figure 5. Coordinate system

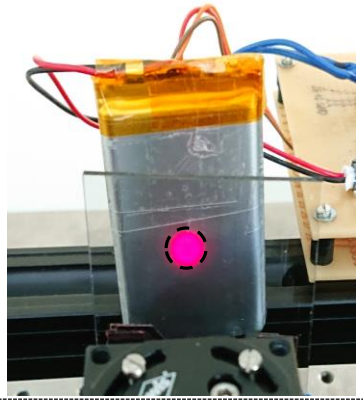

Figure 6. Measuring field on the surface of the battery.

The battery cell is glued to an angle with the flat back (Figure 6). Thus, an increase in the thickness of the cell leads to a shift of the flat front in the Z direction. 3D image processing calculates the thickness change of the battery from the difference of the Z values of the 3D data sets. From the resolution of the translation unit (model M-521.DG, manufacturer Physics Instruments) results a Z resolution of 30nm. The repeatability of the thickness change values for a single pixel is 312nm. It is determined by a measurement series with 25 measurements and is the standard deviation of the Z difference values of the pixels.

The repeatability for the mean thickness change is 64.21nm. It is the standard deviation of the mean Z difference value for a horizontal line of pixels in the X direction with a length of 537 pixels.

During cyclization, the temperature of the battery is measured by a glued-on sensor (model TSIC 506F, manufacturer IST) with an accuracy of 0.1K. A temperature rise from 22.6°C to 29.6°C is measured.

2.1.3. Electronic setup. An electronic setup is used for 100% discharging and charging of the battery and for measuring the amount of charge. To measure the battery voltage, a 16-bit AD converter (model USB 6003, manufacturer National Instruments) is used with a resolution of 0.304mV. The charging and discharging current is measured by means of a current transformer (model LTSR 6-NP, manufacturer LEM) with an accuracy of ± 0.7%. From the current, the charge introduced and removed is calculated by temporal integration. Before starting the measurement, the battery is charged to 4.19V. Discharging takes place via a switchable resistor. Its average current is 1.7A. The electronic discharge protection of the battery responds at 2.75V. This achieves 100% depth of discharge. Charging takes place by the aid of a switchable charge management controller (Model MCP73831/2, manufacturer Microchip) with an average current of 0.37A.

2.2. High precision cell test system

At 30 cycles with 100% DoD the decrease in battery capacity is measured. This is done using a high precision cell test system (Model CTS, manufacturer Basytec) with voltage precision 1mV and current precision 1mA. The four-point measurement method is used to achieve accurate voltage measurement.

3. Results

Figure 7 shows the 3D data set of the 100% charged cell (4.19V).

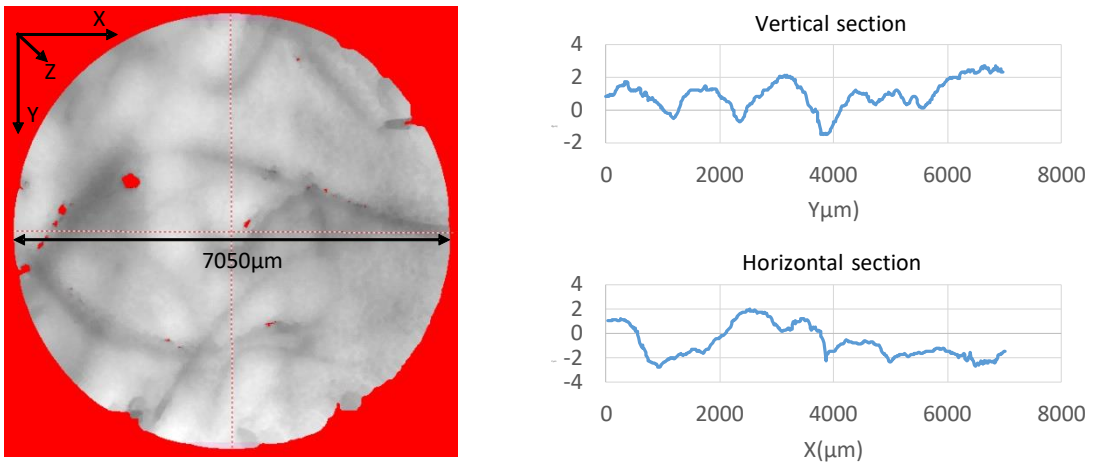

Figure 7. 3D data set of the battery fully charged. The mean Z value is set to zero. The values of the Z values are grey value coded. Pixels without a valid value are highlighted in red. The diameter of the measuring field is 7050µm. The vertical and horizontal sections each contain about 537 values.

The cell surface has a ripple (peak to peak) up to 4µm. Figure 8 shows the difference between the 3D data set of the 100% charged (4.19V) and the 0% charged cell (2.83V). The difference is negative in the coordinate system of the measurement. As expected, the thickness of the battery shrinks during discharge because the volume of the graphite layer shrinks upon discharge. The mean thickness change is 180.6µm. The vertical section through the Z data shows a tilt of the surface of the battery by 6.1µm.

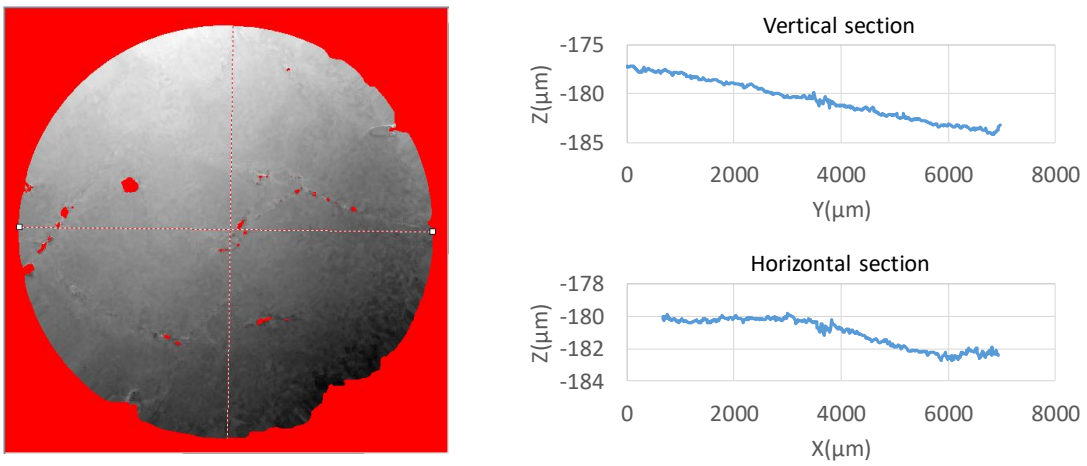

Figure 8. Difference record battery full to record battery empty.

The ratio between the measured value of the average thickness change and the repeatability of the average change in thickness (64.1nm) is thus greater than 2800. Therefore, the measuring principle is suitable for testing cells during production.

There is an approximately linear relationship between the thickness change of the cell and the charge. The deviation of the change in thickness of a straight line is a maximum of 9.3µm during the unloading process (Figure 9). When charging (Figure 10), the deviation from a straight line is a

maximum of 19.1µm. Since interferometer probes can be miniaturized very strongly [16], they can be integrated into the pouch cell. This results in a possible application of interferometers to estimate the state of charge of pouch cells, for example in drones.

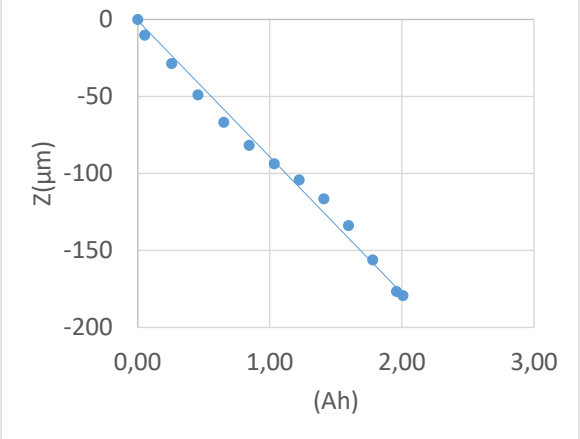

Figure 9. Thickness change and unloaded charge (13 measured values).

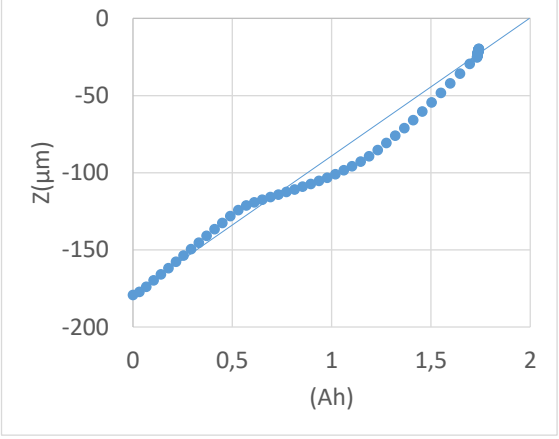

Figure 10. Thickness change and loaded charge (61 measured values).

Figure 11 shows the evolution of cell capacity as measured by the CTS. During the first 5 cycles the capacity increases slightly and then decreases.

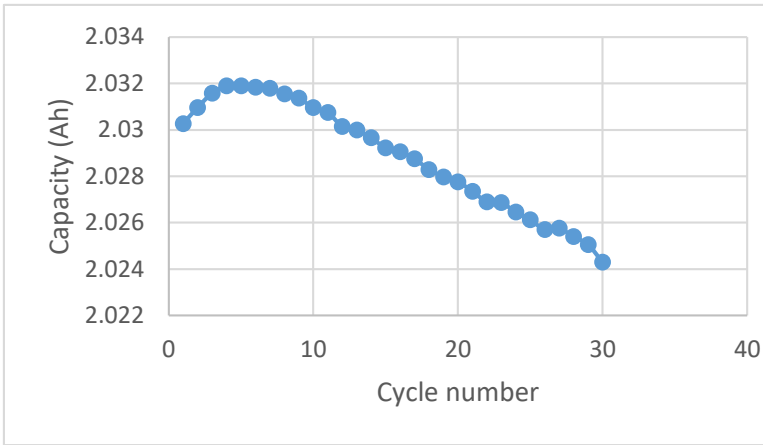

Figure 11. Cell Capacity and number of cycles. The DoD is 100%. The charging current is 1000mA and the discharging current is 400mA. The capacity at cycle number 5 is 2.032Ah. The capacity at cycle number 30 is 2.024Ah.

4. Conclusions

With the interferometric measuring method described in this paper, the change in thickness of pouch cells during charging and discharging can be measured with high precision. An average reduction in the thickness of the cell during unloading by 180.6µm and a tilt of the surface by 6.1µm is measured.

Thickness change of the graphite layer is partly responsible for the decrease in storage capacity over the number of charge and discharge cycles. For the type of cell considered, this decrease is 0.008Ah for 25 cycles. Interferometric measurement of the thickness change is applicable for the estimation of the state of charge of pouch cells or for their quality control in production.

Reference

[1] Mizushima K, Jones P, Wiseman P and Goodenough J 1980 A New Cathode Material For Batteries Of High Energy Density *Materials Res. Bull.* **vol 15** p 783
[2] Mekonnen Y, Sundararajan A and Sarwat A 2016 A Review of Cathode and Anode Materials for Lithium-Ion Batteries *Proc. SoutheastCon (Norfolk VA)*
[3] Rebecca E and Whitacre J 2017 Comparison between Cylindrical and Prismatic Lithium-Ion Cell Costs Using a Process Based Cost Model *J. of Power Sources* **vol 340** p 273
[4] Grandjean T, Anup B, Hosseinzadeh E, Guo Y, McGordon A and Marco J 2017 Large Format Lithium Ion Pouch Cell Full Thermal Characterisation for Improved Electric Vehicle Thermal Management *J. of Power Sources* **vol 359** p 215
[5] Boucar D and Ramchandra P 2014 Potential of Lithium-Ion Batteries in Renewable Energy *Renewable Energy* **vol 76** p 375
[6] Bohn G, Bayer S, Stolz M, Ackva A and Arndt B 2015 Lifetime Simulation of Rechargeable Batteries for Solar Powered Fishing Lights *Proc. 6th RMUTP Int. Conf. (Bangkok)*
[7] Gomez-Camer J, Bünzli C, Hantel M, Poux T and Novak P 2016 On the Correlation between Electrode Expansion and Cycling Stability of Graphite/Si Electrodes for Li-ion Batteries *Carbon* **vol 105** p 42
[8] Jossen A and Weydanz W 2006 *Moderne Akkumulatoren richtig einsetzen* Reichardt Verlag Leipheim und München p 39
[9] Okzuku T, Iwakoshi Y and Sawai K 1993 *Elektrochem. Soc.* **vol 140** p 2490
[10] Okzuku T, Matoba N and Sawai K Direct Evidence on Anomalous Expansion of Grafite-Negative Electrodes on First Charge by Dilatemetry 2001 *J. of Power Sources* **vol 97** p 73
[11] Abbott B et al. 2016 Observation of Gravitational Waves from a Binary Black Hole Merger *Phys. Rev. Lett.* **vol 119** p 061102
[12] Inomata N, Van Toan N, Toda M and Ono T 2018 Evaluation of Piezoresitive Property of Vanadium Oxide Thin Film *IEEE Sensors Lett.* **vol 2**
[13] Miao J, Wang H, Li P, Shen W, Xue C and Xiong J 2016 Glass-SOI-based hybrid-bonded Capacitive Micromachined Ultrasonic Transducer with Hermetic Cavities for Immersion Applications *J. of Micromechanical Systems* **vol 25**
[14] Häusler G, Ettl P, Schenk M, Bohn G and Lazlo I 1999 Limits of Optical Range Sensors and How to Exploit Them *Int. Trends in Optics and Photonics* ed Asakura T (Berlin, Heidelberg: Springer-Verlag) **vol 74** p 328
[15] Sarac Z, Groß R, Richter C, Wiesner B and Häusler G 2004 Optimization of White Light Interferometry on Rough Surfaces Based on Error Analysis *Int. J. for Light and Electron Optics* **vol 115** p 351
[16] Nouira H, Wallerand J, Malak M, Obaton A, Solgado J and Bourouina T 2015 Miniature Silicon Michelson Interferometer Characterization for Dimensional Metrology *Sensors and Actuators* **vol 223** p 141